The Inhibitory Impact of Schisandrin Against LPS-Induced Acute Kidney Injury in Vitro and in Vivo

Weifeng Li
Xi'an Jiaotong University
Qiuxia Huang
Xi'an Jiaotong University
Jinjin Yu
Xi'an Jiaotong University
Jiabao Yu
Xi'an Jiaotong University
Yajie Yang
Xi'an Jiaotong University
Yang Liu
Xi'an Jiaotong University
Huixin Song
Xi'an Jiaotong University
Langjun Cui
Shaanxi Normal University
Xiaofeng Niu (niuxf@mail.xjtu.edu.cn)
Xi'an Jiaotong University https://orcid.org/0000-0002-8349-7010

Research Article

Keywords: Schisandrin, acute kidney injury, inflammation, oxidative stress, macrophages

Posted Date: December 13th, 2021

DOI: https://doi.org/10.21203/rs.3.rs-935326/v1

Abstract

Schisandrin (Sch) is a main bioactive component of *Schisandra sphenanthera Rehd.et Wils*. It has been reported that Sch could regulate inflammatory disease. This study evaluated the anti-inflammatory and anti-oxidant effects effect of Sch on lipopolysaccharide (LPS)-induced macrophages activation and acute kidney injury mice. Male Kunming mice were intraperitoneally injected with LPS (15 mg/kg) after administration of Sch (12.5, 25, 50 mg/kg) seven days for developing acute kidney injury vivo model. RAW264.7 macrophages were pretreatment Sch (10, 20, 40 μM) and administrated LPS (1 μg/ml) to create an in vitro injury model. ELISA results found that Sch administration reduced the production of inflammatory factors induced by LPS in kidney tissues and RAW264.7 macrophages. It has been observed that Sch alleviated oxidative stress by reducing the levels of reactive oxygen species, myeloperoxidase and malondialdehyde, and increasing the activity of superoxide dismutase and glutathione peroxidase. Hematoxylin-eosin staining data suggested that Sch administration significantly reduced inflammatory cell infiltration and the kidney tissue damage induced by LPS. The blood urea nitrogen and creatinine levels were also reduced by Sch treatment. In addition, Western blot and immunohistochemical analysis showed that Sch up-regulated the expression of Nrf2 and HO-1, and decreased the expression of p-p38, p-JNK, p-ERK1/2, p-IκBα, p-NF-κBp65 and TLR4. The current research showed that Sch reduced LPS-induced acute kidney injury by inhibiting inflammation and oxidative stress, and provided insights into potential ways to treat AKI.

1. Introduction

Acute Kidney Injury (AKI) is a common clinical syndrome with kidney function declines rapidly, and accompanied with higher morbidity and mortality [1, 2]. AKI is mainly manifested as abnormal changes in serum creatinine (CRE), urea nitrogen (BUN) and glomerular filtration rate [3]. In recent years, the incidence of acute kidney injury has been steadily increasing [4]. It is more common in hospitalized and critically ill patients and seriously affects the prognosis of patients. It has also become a disease of public health issues affecting global society and economy [5, 6].Therefore, it is very urgent to discover effective drugs for the treatment of acute kidney injury.

Inflammation is a self-defensive physiological response of the immune system to injury and infection. However, inappropriately activated inflammation can become pathogenic inflammatory diseases [7]. Inflammatory storm could be spotted in patients suffering from AKI with a large number of macrophages infiltrated in kidney tissues [8]. Macrophages, as the crucial immune cells, secreted inflammatory cytokines such as tumor necrosis factor-α (TNF-α), interleukin 1β (IL-1β), and interleukin 6 (IL-6), leading to the cascade of other inflammatory cytokines and production of excessive ROS, aggravating tissue damage [9, 10]. These indicated the crucial regulatory role of macrophages in the pathogenesis of AKI.

Lipopolysaccharide (LPS), is a characteristic component of the cell wall of gram-negative bacteria, which was widely used to induce inflammation [11–13]. When induced by LPS, the TLR4 dimer interacts with the downstream adaptor protein to induce MAPK and NF-κB signal transduction [13–15]. Nuclear factor-

κB (NF-κB) is a nuclear transcription factor necessary for the transcription and production of a large number of cytokines [16]. After LPS stimulation, activated NF-κB signaling pathways promote the expression of interleukin-1β (IL-1β), nterleukin-6 (IL-6), tumor necrosis factor-α (TNF-α) and other pro-inflammatory cytokines [17]. These factors promote the entry of macrophages and neutrophils into tissues and organs, causing inflammation [17]. In addition, as one of the most typical signal transduction cascades, the MAPK pathway such as JNK, ERK and p38 MAPK [18] is also involved in the production of various inflammatory mediators in the process of inflammation [19]. Moreover, LPS stimulation induces excessive oxidative stress [20]. The multifunctional regulator nuclear factor erythroid 2 related factor (Nrf2) is a main regulator of cell redox homeostasis activating the expression of antioxidant enzyme genes, such as blood oxygenase-1 (HO-1) [21]. Mounting studies reported that the up-regulation of HO-1 and its products can reduce the production of ROS and inflammatory cytokines in lipopolysaccharide (LPS) stimulated macrophages, thereby regulating oxidative damage and inflammation [22–24].

Schisandra is the dry and mature fruit of *Schisandra sphenanthera Rehd.et Wils*. of the magnolia family *Schisandra sphenanthera* [25]. As the main active component of *schisandra* (see Fig. 1 for the structure), schisandrin (Sch) has multiple effects such as antioxidant, anti-inflammatory and detoxification [26]. However, the effect and mechanisms of Sch on macrophage activation and acute kidney injury remain unclear. Therefore, the study utilized LPS-induced macrophage and acute kidney injury (AKI) mice. The results demonstrated that Sch pretreatment ameliorated LPS-induced macrophage activation and AKI through inhibiting inflammation and oxidative stress.

2. Methods

2.1 Materials and drugs

Sch (purity ≥ 98%) was provided by Baoji Chenguang Biotechnology Co., Ltd. (Shanxi, China) and was confirmed by the Pharmaceutical and Post-Laboratory of School of Medicine, Xi'an Jiaotong University (Xi'an, China). Dexamethasone (DEX), as a positive drug, was purchased from Zhejiang Xianju Pharmaceutical Co., Ltd. (Zhejiang, China). Lipopolysaccharide (LPS, Escherichia coli with serotype O55:B5), purchased from Sigma (St. Louis, MO, USA). DMEM and fetal bovine serum (FBS) were purchased from Gibco (Gibco-BRL, Gaithersburg, MD, USA). Serum Cystatin C (sCysC), TNF-α, IL-1β and IL-6 enzyme-linked immunosorbent assay (ELISA) kits were provided by Bio Swamp Life Science Lab for the determination of related factors in mice. The BUN, CRE, Myeloperoxidase (MPO), malondialdehyde (MDA), superoxide dismutase (SOD) and glutathione peroxidase (GSH) test kits were purchased from Nanjing Jiancheng Bioengineering Institute. Primary antibodies (TLR4, Nrf2, HO-1, p-ERK1/2, p-JNK1/2, NF-κBp65 and β-actin) were purchased from ABclonal (Boston, MA, USA). ERK1/2, JNK1/2, p-NF-κBp65, p-p38 and p38 antibodies were purchased from Bioss (Santa Cruz, California, USA). HRP Goat Anti-Rabbit IgG (secondary antibody) was obtained from ABclonal in the United States.

2.2 In Vitro

2.2.1 Cell culture

RAW 264.7 macrophages were incubated in DMEM medium supplemented with 10% fetal bovine serum (FBS) in an incubator at 37°C and 5% CO2. In the AKI group, the cells were treated with LPS (10 μg/mL) for 24 h. Sch was dissolved in dimethyl sulfoxide (DMSO; Sigma-Aldrich) and adjusted to the final concentrations (10, 20 and 40 μM) using complete DMEM medium. Before LPS treatment, the administration group received different doses of Sch treatment.

2.2.2 Cell viability assay

MTT was used to detect the effect of different concentrations of Sch on RAW 264.7 macrophages to select the appropriate concentration. Cells in good condition were inoculated into a 96-well plate (1×104/well), and incubated with 180 μL of medium. After 24 h, the cells were treated with Sch (0, 1.25, 2.5, 5, 10, 20, 40, 80, and 160 μM) and cultured for 24 h. Carefully removed the supernatant from the well plate, and added 20 μL MTT solution (0.5 mg/mL) to each well and incubated for 4 h. The purple MTT formazan was solubilized with 180 μL DMSO/well, and measured the OD value at 490 nm by a microplate reader (BioTek ELx800, USA).

2.2.3 IL-6 and monocyte chemotactic protein-1 (MCP-1) production in RAW 264.7 macrophages

The release of IL-6 and MCP-1 was determined using the ELISA assay kit. In brief, the RAW246.7 cells were cultured in 96-well plates and incubated with in DMEM containing different concentrations of Sch and LPS for 12 h respectively. Using a microplate reader to determine the OD value of cytokine levels according to the manufacturer's instructions.

2.2.4 Measurement of ROS levels in RAW 264.7 macrophages

RAW264.7 macrophages were treated with different concentrations of Sch (10, 20, 40 μM) for 24 h, and then incubated with LPS (1 μg/ml) for 24 h. After discarding the cell culture supernatant, 10 μM DCFH-DA was added and incubated at 37°C for 1 h. After washing several times with PBS, the intracellular reactive oxygen species production was observed and imaged using a fluorescence microscope (Nikon, Tokyo, Japan).

2.3 In Vivo

Male Kunming mice (18–22 g, n = 60) with an average age of 8 weeks were purchased from the Animal Experiment Center of Xi'an Jiaotong University (Shanxi Province, China). Before treatment, all mice had free access to water and food in the animal room, and adapt to the environment under pathogen-free conditions of 12 h of light and 12 h of darkness every day. There were five animals in each cage. This study was conducted in accordance with the experimental protocol approved by the Institutional Animal Genetics Committee of Xi'an Jiaotong University.

2.3.1 Mice model of LPS-induced AKI and drug administration

AKI was induced by LPS. After a three-day adaptation period, the mice were randomly divided into six experimental groups (ten mice in each group), namely control group, AKI group (LPS with 15 mg/kg), Sch (12.5, 25 and 50 mg/kg) + LPS group, and DEX + LPS group. Sch was dissolved in 0.1% Tween and prepared dosing solutions with final concentrations of 12.5 mg/kg, 25 mg/kg and 50 mg/kg using 2% sodium carboxymethyl cellulose. Before the administration of LPS, mice in the (Sch + LPS) group and (DEX + LPS) group were fed Sch and DEX for 7 days, respectively. On the seventh day, 6 h after intraperitoneal injection of LPS (except the control group), blood was taken from the eyeballs to determine factors, and then the mice were sacrificed and two kidneys were taken out for further analysis (hematoxylin-eosin (H&E) staining and immunohistochemistry test).

2.3.2 Determination of inflammatory cytokines in the tissue

The levels of TNF-α, IL-6, IL-1β in the rice serum were detected by ELISA kits. According to the manufacturer's agreement, continuously added working reagents, and readed the optical density (OD) of each microcell at 450 nm with a microplate reader (Bio-Tek ELx800, USA).

2.3.3 Assay of tissue CRE, BUN and Serum Cystatin C (sCysC)

Kidney function was assessed by CRE, BUN and sCysC using commercial kits purchased from Nanjing Jiancheng Institute of Biological Engineering. According to the instructions of the kit, 100 mg of tissue was weighed and physiological saline was added to prepare a 10% tissue homogenate. Used the corresponding working solution in turn and incubated at 37°C, and then measured the optical density (OD) at 450 nm in a microplate reader (Bio-Tek ELx800, USA).

2.3.4 Oxidative stress in the kidney

To evaluate the oxidative stress and antioxidant markers in kidney tissue of different treatment groups. According to a certain ratio, the kidney tissues were dissolved in physiological saline to prepare a 10% tissue homogenate. The levels of MDA, MPO, SOD and GSH-Px were measured by the instructions of the test kit to assess the tissue damage of the kidney.

2.3.5 Histopathological examination

For routine analysis, the collected fresh kidney tissues were fixed with 4% paraformaldehyde for 48 h, and dehydrated with different concentrations of ethanol and xylene. Next, the sample embedded in paraffin at 60°C, and sliced into 5 um thick sections. Then, the tissues were deparaffinized and stained with H&E according to standard histopathology protocol. The degree of kidney damage was observed under an optical microscope (Olympus Optical, Tokyo, Japan). Moreover, 0 means no damage; 1 means mild damage; 2 means moderate damage; 3 means severe damage; 4 means that the degree of damage is very severe as the standard to evaluate kidney damage.

2.3.6 Immunohistochemistry

Using immunohistochemistry experiments to evaluate protein expression in kidney tissue. The kidney tissue sections were deparaffinized and rehydrated with xylene, absolute ethanol, double distilled water and PBS, and antigen retrieval solution (citrate buffer) was added for antigen retrieval. Then, 3% H2O2 was used to block the activity of endogenous peroxidase and incubated with goat serum for 10 minutes at 37°C for blocking. The tissue sections were incubated with phosphorylated JNK1/2, HO-1, and NF-κBp65 antibodies overnight at 4°C, and then incubated with horseradish peroxidase-conjugated secondary antibodies for 30 min at 37°C. Staining with DAB and counterstain with hematoxylin. The sections were observed using an Olympus DP-71 microscope equipped with a digital camera. Finally, the results were semi-quantitatively evaluated based on the percentage of positive cells in ten random images viewed at x200 magnification.

2.3.7 Western blotting

The quantified kidney tissue was lysed with RIPA lysis buffer to prepare a tissue homogenate and the supernatant was collected by centrifugation (1000 r/min). The BCA kit were used to detect the protein concentration to determine the loading amount. Separated the same amount of protein with a 10% SDS-polyacrylamide electrophoresis gel, and then transferred it to a PVDF membrane. After blocking with 5% fat-free milk powder at room temperature for 2 h, incubated the membrane with primary antibodies overnight (4°C). The next day, the blots were incubated with the secondary antibodies for 1 h (37°C) and used the ECL blot analysis kit to generate a positive signal. Analyze and quantify the intensity of protein bands by luminescence imaging system to detect total protein density.

2.4 Statistical analyses

Statistical analysis was performed using Graph Pad Prism 5.0 and all data were expressed as mean ± SEM. A one-way analysis of variance (ANOVA) and Dennett post-inspection were used to determine the statistical difference between multiple groups with $P < 0.05$ as the standard.

3. Results

3.1 Effect of Sch on the toxicity of RAW 264.7 macrophages

The MTT assay was used to detect the effect of Sch on the survival rate of RAW264.7 macrophages. The results (Fig. 1B) showed that compared with the control group, when the cells were pretreated with Sch of 1.25 to 80 μM, there was no significant change in cell viability. However, Sch at 160 μM significantly inhibited cell viability ($P < 0.01$). Therefore, we decided to choose 10, 20, and 40 μM Sch for subsequent cell research.

3.2 Effect of Sch on LPS-induced RAW264.7 macrophages cytokine production

As shown in Fig. 1C and 1D, the effect of Sch on the expression of inflammatory factors IL-6 and MCP-1 in RAW264.7 macrophages. To verify the effect of Sch in vitro, LPS were used to process RAW264.7 macrophages. Compared with the control group, the levels of IL-6 and MCP-1 in cells were significantly increased after LPS stimulation ($P < 0.01$). However, compared with the high expression (160 ± 1.79 pg/ml, 450 ± 21.6 pg/ml) in the LPS group, the expression levels of IL-6 and MCP-1 decreased to 87.0 ± 9.58 pg/ml and 216 ± 5.81 pg/ml at the Sch dose of 40 μM, respectively ($P < 0.001$). The results showed that Sch has an inhibitory effect on the production of IL-6 and MCP-1 in RAW264.7 macrophages stimulated by LPS.

3.3 Effect of Sch on the activation of ROS in RAW264.7 macrophages

ROS are widely known to be related to the intensity of oxidative stress in cellular responses. In the AKI group, the green fluorescence intensity increased significantly, indicating that the production of ROS in the cells increased ($P < 0.001$). The production of ROS in the administration group was significantly reduced ($P < 0.01$), which indicated that Sch was able to inhibit the production of oxidative stress by suppressed the activation and production of ROS (Fig. 2A-B).

3.4 Effect of Sch on Nrf2/HO-1 signaling pathway in RAW264.7 macrophages

The Nrf2 pathway is involved in the occurrence and development of cellular oxidative stress. It was still unknown if Nrf2 pathway was involved in the roles of Sch in LPS-stimulated RAW264.7 macrophages. Therefore, western blot was performed to further explore the effect of Sch and Nrf2 inhibitor luteolin on Nrf2 /HO-1signaling pathway-related proteins expressions. From the results, we found that Sch treatment significantly increased Nrf2 and HO-1 expressions, while luteolin inhibited the production of these proteins. In addition, Sch still up-regulated the expression of Nrf2 and HO-1 under the premise that luteolin exerts an inhibitory effect. These data means that Sch can inhibit the production of LPS-induced oxidative stress in RAW246.7 cells by participating in the activation of Nrf2/HO-1.

3.4 Effect of Sch on the inflammatory response in serum

Results for TNF-α, IL-6, and IL-1β are shown in Fig. 3. The concentrations of inflammatory cytokine TNF-α (268 ± 2.34 pg/ml) in the LPS stimulated group were significantly enhanced compared with the control group (154 ± 3.76 pg/ml, $P < 0.001$) (Fig. 3A). In the (LPS + Sch) group, the secretion of TNF-α was reduced ($P < 0.01$). As shown in Fig. 3B and 3C, compared with the control group (80.9 ± 5.62 pg/ml, 144 ± 6.59 pg/ml respectively), the IL-1β level (232 ± 15.9 pg/ml) and IL-6 level (340 ± 20.4 pg/ml) were increased in mice after LPS stimulation ($P < 0.001$). Incubation with Sch attenuated the presence of LPS-induced IL-6 and IL-1β in a concentration-dependent manner, in which Sch of 50 mg/kg reduced the contents of IL-6 and IL-1β induced by LPS by 181 pg/ml, 123 pg/ml respectively ($P < 0.01$).

3.5 Effects of Sch on the content of CRE, BUN and sCysC in the kidney tissues

To roughly assess the kidney damage in mice, the content of BUN and CRE in the kidney tissue were measured. As shown in Fig. 4A, in the LPS-induced AKI group, the levels of CRE were significantly increased by 3-fold ($P < 0.001$) compared with the control group. On the other hand, compared with the LPS group, the administration group (receiving 50 mg/kg of Sch pretreatment) reduced the activity of CRE in mice kidney tissue by 35.2 μmol/L ($P < 0.001$). Compared with control mice (27.9 ± 0.158 mmol/L), LPS significantly enhanced the activity of BUN (54.3 ± 2.60 mmol/L) in mice ($P < 0.001$), while BUN activity was significantly down-regulated at the Sch concentration of 12.5, 25 and 50 mg/kg ($P < 0.01$, Fig. 4B).

At the same time, changes in sCysC levels were also tested in experiments to assess the effect of Sch on kidney function. As shown in Fig. 4C, LPS induced overexpression of sCysC ($P < 0.01$), which increased 0.477 ng/ml compared to the control group. However, Sch and DEX pretreatment significantly reduced the level of sCysC in mice serum ($P < 0.05$). Moreover, this study also used H&E staining to assess the degree of kidney damage. As shown in Fig. 4D, in the kidneys of the LPS group, inflammatory cell infiltration, disappearance of brush border and destruction of glomerular structure were observed. However, the pretreatment with Sch at doses of 12.5, 25, or 50 mg/kg and DEX at 5 mg/kg significantly reduced the pathological changes caused by LPS. In general, Sch pretreatment can effectively inhibit the production of these inflammatory factors by LPS.

3.6 Effect of Sch on the MDA, SOD, MPO and GSH-Px levels in the kidney tissues

Kunming mice were pretreated with different concentrations of Sch and a certain dose of DEX, and then stimulated with 25mg/kg LPS for 6 h. As shown in Fig. 5A-B, GSH-Px and SOD levels activity were decreased in the LPS-induced AKI group ($P < 0.05$). In contrast, pretreatment with Sch (12.5, 25, and 50 mg/kg) and DEX significantly increased the SOD and GSH-Px content ($P < 0.05$). In addition, the activity of MDA and MPO were detected in kidney tissue. Compared with the control group (1.06 ± 0.048 nmol/mg prot and 0.234 ± 0.0078 U/g), mice tissues in the LPS group ($P < 0.01$) had higher levels of MDA (2.68 ± 0.023 nmol/mg prot) and MPO (0.314 ± 0.0029 U/g). However, the Sch group showed a significant down-regulation of the activities of MDA and MPO by 0.09734 U/g, 0.1298 U/g, 0.1534 U/g ($P < 0.001$) at concentrations of 12.5, 25 and 50 mg/kg (Fig. 5C-D).

3.7 Sch activated the Nrf2/HO-1 signaling pathway in the kidney

This experiment evaluated the role of Nrf2/HO-1 pathway in kidney protection. In order to verify the expression of Nrf2 and HO-1 in mice kidney tissue induced by LPS, it was pretreated with different concentrations of Sch and DEX, then stimulated with LPS and measured protein expression (Fig. 6A). Induction of LPS resulted in a significant decrease in the expression of Nrf2 and HO-1 protein compared to the control group ($P < 0.01$). On the contrary, the protein levels of Nrf2 and HO-1 in the administration of Sch (50 mg/kg) showed an apparent increase, and the expression of HO-1 approached the level of the control group ($P < 0.05$). In addition, the results of immunohistochemistry further showed that

pretreatment with Sch can boost the expression of HO-1 protein ($P < 0.05$, Fig. 6B). Our research showed that Sch can inhibit the activation of Nrf2/HO-1 signaling pathway induced by LPS.

3.8 Sch inhibited NF-κB and MAPK proteins expression in the kidney

NF-κB signaling pathway plays a key role in the inflammatory response. This study tested the expression of NF-κB signaling pathway. The results of the Western blot in Fig. 7A showed that the expression of p-NF-κBp65, p-IκBα and TLR4 in the LPS group were significantly higher than that in the control group, increasing by 50%, 63% and 68% ($P < 0.001$). By contrast, the protein concentration after administration of Sch was decreased ($P < 0.01$). The results showed that Sch reduced the expression of NF-κB pathway protein stimulated by LPS. In order to further investigate the anti-inflammatory effects of Sch, western blot was also performed to detect the expression of key proteins related to the MAPK pathway. LPS stimulation significantly upregulated the levels of p-JNK1/2, p-ERK1/2 and p-P38 ($P < 0.001$), and Sch treatment attenuated this change. At the dose of Sch was 50 mg/kg, the protein expression of p-ERK and p-JNK decreased to a level close to that of the control group ($P < 0.05$, Fig. 7B). Immunohistochemical analysis further proved the role of Sch. These results showed that Sch effectively reduced the proteins expression ($P < 0.01$) of the NF-κB and MAPK pathway in kidney tissue (Fig. 8).

4. Discussion

Inflammatory diseases are known to be caused by excess inflammatory responses and oxidative stress [27]. In this study, we described the anti-inflammatory and anti-oxidative activity of Sch in LPS-induced macrophage and acute kidney injury in mice.

LPS administration may induce systemic inflammation reaction, and increase the number of neutrophils and accelerate the release of cytokines and and inflammatory mediators ,including IL-1β, IL-6, MCP-1 and TNF-α [28]. Their overproduction can amplify inflammation and cause tissue damage [29, 30]. Moreover, CRE, BUN and sCysC are widely used as markers to assess kidney function, which were used for early detection of AKI[31, 32]. CRE, BUN and sCysC levels tend to increase due to kidney abnormalities induced by LPS administration [33]. In addition, LPS also induce kidney pathological alterations, such as inflammatory cell infiltration. In this study, we found that the levels of these pro-inflammatory mediators in LPS-induced RAW264.7 cells and acute kidney injury mice were significantly decreased in Sch pretreatment group. Additionally, Sch significantly reduce the increased levels of BUN, sCysC and CRE in the mice with LPS stimulation. We also found that Sch clearly relieved inflammatory infiltration of kidney tissues. Based on the above results, it may be concluded that Sch plays an anti-inflammatory effect by inhibiting the expression of pro-inflammatory factors and kidney tissue damage, and then controls the activation of macrophages and the progression of acute kidney injury.

According to literatures, NF-κB and MAPK are involved in the occurrence and development of innate immunity and inflammation, and also regulated the production of numerous pro-inflammatory chemokines and cytokines[34]. To study the mechanism of Sch in regulating LPS-induced kidney injury,

we detected components of MAPK and NF-κB signaling pathways. In the present study, NF-κB pathway were notably activated by LPS in kidney tissues. However, Sch pretreatment decreased the expression levels ofp-NF-κBp65 and p-IκBα and TLR4. This indicated that NF-κB signaling activation mediates the anti-inflammatory effect of Sch in AKI mice. Moreover, the activation of MAPKs also promote the release of large number of inflammatory mediators [35]. Among them, the ERK signaling pathway is involved in cell proliferation and differentiation, while the JNK and p38 MAPK pathways mainly mediate pro-inflammatory mediators and regulate cell apoptosis [36]. Therefore, this study examined whether Sch can block the MAPK inflammatory pathway in mice with LPS-induced acute kidney injury. As expected, activated p-p38, p-ERK1/2 and p-JNK1/2 were partially down-regulated by Sch. In general, pretreatment of Sch attenuated TLR4-mediated activation of MAPKs and NF-κB, and further modulated the production of pro-inflammatory mediators and reduced kidney damage to inhibit the inflammatory response of AKI.

Oxidative stress are the key pathophysiological processes in the progress of kidney injury [37]. Studies have reported that LPS could promote the up-regulation of oxidative stress in tissues [38]. The formation of MDA and the enhancement of MPO activity will accelerate the infiltration of neutrophils in the kidney tissue and promote the progress of inflammation [38] [39]. As effective antioxidants, SOD and GSH-Px are equally important in response to oxidative stress and regulating the redox state of cells[37, 40–42]. Studies also showed that Nrf2, an important antioxidant pathway, protect cells from inflammation through regulation of oxidative stress [43]. It also regulates the expression of the antioxidant enzyme HO-1 in macrophages[44]. The up-regulation of HO-1 can reduce the release of ROS and inflammatory cytokines, thereby protecting tissues from damage [23]. Our data showed that Nrf2 protein expression increased after Sch pretreatment and activated the Nrf2/HO-1 pathway, which upregulated the expression of downstream antioxidant HO-1 protein. Moreover, Sch also prevented the LPS-induced decreases in SOD and GSH-Px levels and the increases in MDA and MPO levels in the kidney tissue of AKI mice. These results indicated that Sch can reduce the kidney damage caused by oxidative stress through up-regulating the Nrf2/HO-1 signaling pathway. In the current study, we also observed that Sch inhibited production of ROS in LPS-treated RAW264.7 cells at a dosage-dependent manner. These data further provided the evidence for the protective effect of Sch in LPS-induced AKI, namely the anti-oxidative stress effect of Sch.

In conclusion, Sch have a great preventive effect on LPS-induced AKI. These beneficial effects are closely related to anti-inflammatory and anti-oxidative stress pathways. These findings strongly suggest that Sch could be a potential medicine for the treatment of LPS-induced AKI in the future. However, there are some limitations in this paper. The LPS-induced AKI mice model could not mimic all aspects of the human conditions and need further studies to the potential role of Sch in LPS-induced human kidney macrophages.

Declarations

Data Availability

The data supporting the findings of this study are available within the article and material.

Author information

Affiliations

School of Pharmacy, Xi'an Jiaotong University, No. 76 Western Yanta Road, Xi'an City, Shaanxi Province 710061, P.R China.

Weifeng Li, Qiuxia Huang, Jinjin Yu, Jiabao Yu, Yajie Yang, Yang Liu, Huixin Song, Xiaofeng Niu

School of Life Sciences , Shaanxi Normal University , Xi'an, P.R. China.

Langjun Cui

Contributions

Weifeng Li: Writing-Original draft preparation, Writing-Review & Editing, Investigation, Methodology; Qiuxia Huang: Methodology, Writing- Original draft preparation, Writing-Review & Editing, Data curation; Jinjin Yu: Valization; Jiabao Yu: Formal analysis; Yajie Yang: Software; Yang Liu: Valization; Huixin Song: Software. Xiaofeng Niu and Langjun Cui: Conceptualization, Funding acquisition, Supervision, Resources.

Corresponding author

Xiaofeng Niu, School of Pharmacy, Xi'an Jiaotong University, No. 76 Western Yanta Road, Xi'an City, Shaanxi Province 710061, P.R China. E-mail: niuxf@mail.xjtu.edu.cn

Langjun Cui, School of Life Sciences , Shaanxi Normal University , Xi'an, P.R. China. E-mail: ljcui@snnu.edu.cn

Ethics declarations

Ethics Approval and Consent to Participate

All experimental operations were performed in accordance with the National Institutes of Health (NIH) Laboratory Animal Care and Use Guidelines and approved by the Ethics Committee of Xi'an Jiaotong University(Permit No. XJTU 2019–003).

Consent for Publication

Not applicable.

Conflict of Interest

The authors declare no conflict of interest.

Acknowledgements

This work was supported by Project of National key R & D plan (no.: 2019YFC1712606) and Project of Shaanxi Traditional Chinese Medicine Administration (no.: 2019-13)(PR China).

References

1. Koeze J, Keus F, Dieperink W, van der Horst IC, Zijlstra JG, van Meurs M. Incidence, timing and outcome of AKI in critically ill patients varies with the definition used and the addition of urine output criteria. BMC Nephrol 2017; 18:70.
2. Sharawy MH, Serrya MS. Pirfenidone attenuates gentamicin-induced acute kidney injury by inhibiting inflammasome-dependent NLRP3 pathway in rats. Life Sci 2020; 260:118454.
3. Jacob J, Dannenhoffer J, Rutter A. Acute Kidney Injury. Primary Care: Clinics in Office Practice 2020; 47:571-584.
4. Levey AS, James MT. Acute Kidney Injury. Ann Intern Med 2017; 167:ITC66-ITC80.
5. Lewington AJ, Cerda J, Mehta RL. Raising awareness of acute kidney injury: a global perspective of a silent killer. Kidney Int 2013; 84:457-67.
6. Mehta RL, Cerdá J, Burdmann EA, Tonelli M, García-García G, Jha V, et al. International Society of Nephrology's 0by25 initiative for acute kidney injury (zero preventable deaths by 2025): a human rights case for nephrology. The Lancet 2015; 385:2616-2643.
7. Dong J. Signaling Pathways Implicated in Carbon Nanotube-Induced Lung Inflammation. Front Immunol 2020; 11:552613.
8. Shu B, Feng Y, Gui Y, Lu Q, Wei W, Xue X, et al. Blockade of CD38 diminishes lipopolysaccharide-induced macrophage classical activation and acute kidney injury involving NF-kappaB signaling suppression. Cell Signal 2018; 42:249-258.
9. Qiu P, Liu Y, Zhang J. Review: the Role and Mechanisms of Macrophage Autophagy in Sepsis. Inflammation 2019; 42:6-19.
10. Jafarzadeh A, Chauhan P, Saha B, Jafarzadeh S, Nemati M. Contribution of monocytes and macrophages to the local tissue inflammation and cytokine storm in COVID-19: Lessons from SARS and MERS, and potential therapeutic interventions. Life Sci 2020; 257:118102.
11. Tufvesson-Alm M, Imbeault S, Liu XC, Zheng Y, Faka A, Choi DS, et al. Repeated administration of LPS exaggerates amphetamine-induced locomotor response and causes learning deficits in mice. J Neuroimmunol 2020; 349:577401.
12. Zhu C, Zhou J, Li T, Mu J, Jin L, Li S. Urocortin participates in LPS-induced apoptosis of THP-1 macrophages via S1P-cPLA2 signaling pathway. Eur J Pharmacol 2020; 887:173559.
13. Schweikl H, Birke M, Gallorini M, Petzel C, Bolay C, Waha C, et al. HEMA-induced oxidative stress inhibits NF-kappaB nuclear translocation and TNF release from LTA- and LPS-stimulated immunocompetent cells. Dent Mater 2021; 37:175-190.

14. Schmalz G, Krifka S, Schweikl H. Toll-like receptors, LPS, and dental monomers. Adv Dent Res 2011; 23:302-6.
15. Wu H, Wang Y, Zhang Y, Xu F, Chen J, Duan L, et al. Breaking the vicious loop between inflammation, oxidative stress and coagulation, a novel anti-thrombus insight of nattokinase by inhibiting LPS-induced inflammation and oxidative stress. Redox Biol 2020; 32:101500.
16. De Kozak Y, Thillaye-Goldenberg B, Naud MC, Da Costa AV, Auriault C, Verwaerde C. Inhibition of experimental autoimmune uveoretinitis by systemic and subconjunctival adenovirus-mediated transfer of the viral IL-10 gene. Clin Exp Immunol 2002; 130:212-23.
17. Lai JL, Liu YH, Liu C, Qi MP, Liu RN, Zhu XF, et al. Indirubin Inhibits LPS-Induced Inflammation via TLR4 Abrogation Mediated by the NF-kB and MAPK Signaling Pathways. Inflammation 2017; 40:1-12.
18. Udompong S, Mankhong S, Jaratjaroonphong J, Srisook K. Involvement of p38 MAPK and ATF-2 signaling pathway in anti-inflammatory effect of a novel compound bis[(5-methyl)2-furyl](4-nitrophenyl)methane on lipopolysaccharide-stimulated macrophages. Int Immunopharmacol 2017; 50:6-13.
19. Koga Y, Tsurumaki H, Aoki-Saito H, Sato M, Yatomi M, Takehara K, et al. Roles of Cyclic AMP Response Element Binding Activation in the ERK1/2 and p38 MAPK Signalling Pathway in Central Nervous System, Cardiovascular System, Osteoclast Differentiation and Mucin and Cytokine Production. Int J Mol Sci 2019; 20.
20. Park HJ, Gholam Zadeh M, Suh JH, Choi HS. Dauricine Protects from LPS-Induced Bone Loss via the ROS/PP2A/NF-kappaB Axis in Osteoclasts. Antioxidants (Basel) 2020; 9:588.
21. Loboda A, Damulewicz M, Pyza E, Jozkowicz A, Dulak J. Role of Nrf2/HO-1 system in development, oxidative stress response and diseases: an evolutionarily conserved mechanism. Cell Mol Life Sci 2016; 73:3221-47.
22. Luo D, Guo Y, Cheng Y, Zhao J, Wang Y, Rong J. Natural product celastrol suppressed macrophage M1 polarization against inflammation in diet-induced obese mice via regulating Nrf2/HO-1, MAP kinase and NF-κB pathways. Aging (Albany NY) 2017; 9:2069-2082.
23. Mohan S, Gupta D. Crosstalk of toll-like receptors signaling and Nrf2 pathway for regulation of inflammation. Biomed Pharmacother 2018; 108:1866-1878.
24. Hong C, Cao J, Wu CF, Kadioglu O, Schuffler A, Kauhl U, et al. The Chinese herbal formula Free and Easy Wanderer ameliorates oxidative stress through KEAP1-NRF2/HO-1 pathway. Sci Rep 2017; 7:11551.
25. Niu J, Xu G, Jiang S, Li H, Yuan G. In Vitro Antioxidant activities and anti-diabetic effect of a polysaccharide from Schisandra sphenanthera in rats with type 2 diabetes. Int J Biol Macromol 2017; 94:154-160.
26. Szopa A, Ekiert R, Ekiert H. Current knowledge of Schisandra chinensis (Turcz.) Baill. (Chinese magnolia vine) as a medicinal plant species: a review on the bioactive components, pharmacological properties, analytical and biotechnological studies. Phytochem Rev 2017; 16:195-218.

27. Delgado-Roche L, Mesta F. Oxidative Stress as Key Player in Severe Acute Respiratory Syndrome Coronavirus (SARS-CoV) Infection. Arch Med Res 2020; 51:384-387.
28. Gao H, Kang N, Hu C, Zhang Z, Xu Q, Liu Y, et al. Ginsenoside Rb1 exerts anti-inflammatory effects in vitro and in vivo by modulating toll-like receptor 4 dimerization and NF-kB/MAPKs signaling pathways. Phytomedicine 2020; 69:153197.
29. Jiang K, Chen X, Zhao G, Wu H, Mi J, Qiu C, et al. IFN-τ Plays an Anti-Inflammatory Role in Staphylococcus aureus-Induced Endometritis in Mice Through the Suppression of NF-κB Pathway and MMP9 Expression. J Interferon Cytokine Res 2017; 37:81-89.
30. Rull A, Beltran-Debon R, Aragones G, Rodriguez-Sanabria F, Alonso-Villaverde C, Camps J, et al. Expression of cytokine genes in the aorta is altered by the deficiency in MCP-1: effect of a high-fat, high-cholesterol diet. Cytokine 2010; 50:121-8.
31. Kagawa T, Zarybnicky T, Omi T, Shirai Y, Toyokuni S, Oda S, et al. A scrutiny of circulating microRNA biomarkers for drug-induced tubular and glomerular injury in rats. Toxicology 2019; 415:26-36.
32. Liu J. Evaluation of serum cystatin C for diagnosis of acute rejection after renal transplantation. Transplant Proc 2012; 44:1250-3.
33. Shi L, Zhang Y, Xia Y, Li C, Song Z, Zhu J. MiR-150-5p protects against septic acute kidney injury via repressing the MEKK3/JNK pathway. Cell Signal 2021; 86:110101.
34. Zhao H, Wu L, Yan G, Chen Y, Zhou M, Wu Y, et al. Inflammation and tumor progression: signaling pathways and targeted intervention. Signal Transduct Target Ther 2021; 6:263.
35. Hu Q, Wang H, He C, Jin Y, Fu Z. Polystyrene nanoparticles trigger the activation of p38 MAPK and apoptosis via inducing oxidative stress in zebrafish and macrophage cells. Environ Pollut 2021; 269:116075.
36. Elghobashy YA, Assar MF, Mahmoud AA, Monem AEA, Elmasry S. The relation between mitogen activated protein kinase (MAPK) pathway and different genes expression in patients with beta Thalassemia. Biochem Biophys Rep 2020; 24:100836.
37. Lv H, Liu Q, Wen Z, Feng H, Deng X, Ci X. Xanthohumol ameliorates lipopolysaccharide (LPS)-induced acute lung injury via induction of AMPK/GSK3beta-Nrf2 signal axis. Redox Biol 2017; 12:311-324.
38. Pavlakou P, Liakopoulos V, Eleftheriadis T, Mitsis M, Dounousi E. Oxidative Stress and Acute Kidney Injury in Critical Illness: Pathophysiologic Mechanisms-Biomarkers-Interventions, and Future Perspectives. Oxid Med Cell Longev 2017; 2017:6193694.
39. Yu JT, Hu XW, Chen HY, Yang Q, Li HD, Dong YH, et al. DNA methylation of FTO promotes renal inflammation by enhancing m(6)A of PPAR-α in alcohol-induced kidney injury. Pharmacol Res 2021; 163:105286.
40. Aoki K, Yanazawa K, Tokinoya K, Sugasawa T, Suzuki T, Yoshida Y, et al. Renalase is localized to the small intestine crypt and expressed upon the activation of NF-kappaB p65 in mice model of fasting-induced oxidative stress. Life Sci 2021; 267:118904.
41. Hybertson BM, Gao B, Bose SK, McCord JM. Oxidative stress in health and disease: the therapeutic potential of Nrf2 activation. Mol Aspects Med 2011; 32:234-46.

42. Kartha RV, Terluk MR, Brown R, Travis A, Mishra UR, Rudser K, et al. Patients with Gaucher disease display systemic oxidative stress dependent on therapy status. Mol Genet Metab Rep 2020; 25:100667.
43. Lee JH, Jo EH, Lee B, Noh HM, Park S, Lee YM, et al. Soshiho-Tang, a Traditional Herbal Medicine, Alleviates Atopic Dermatitis Symptoms via Regulation of Inflammatory Mediators. Front Pharmacol 2019; 10:742.
44. Rossi M, Korpak K, Doerfler A, Zouaoui Boudjeltia K. Deciphering the Role of Heme Oxygenase-1 (HO-1) Expressing Macrophages in Renal Ischemia-Reperfusion Injury. Biomedicines 2021; 9.

Figures

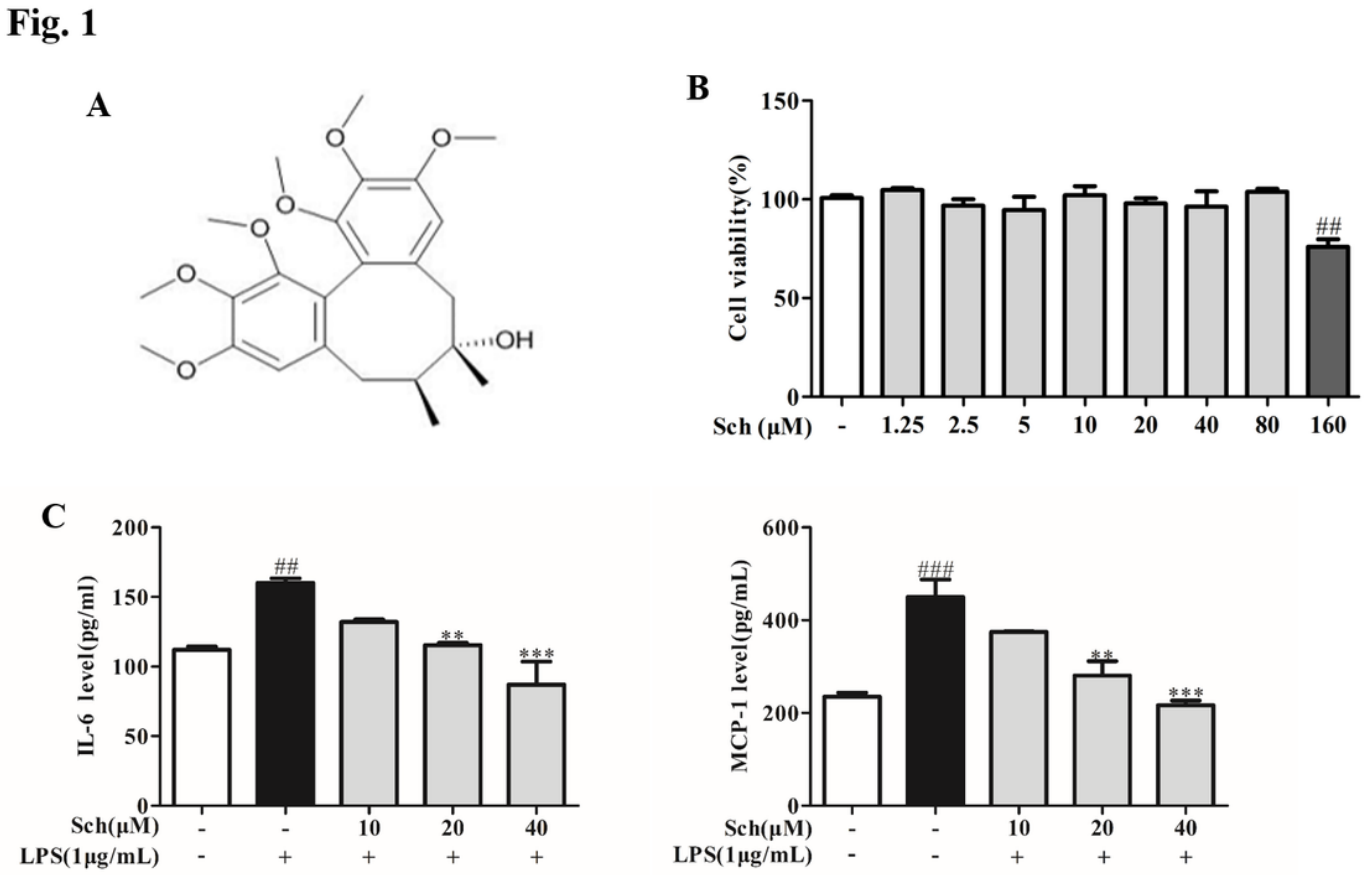

Figure 1

The chemical structure of schisandrin.

Fig. 2

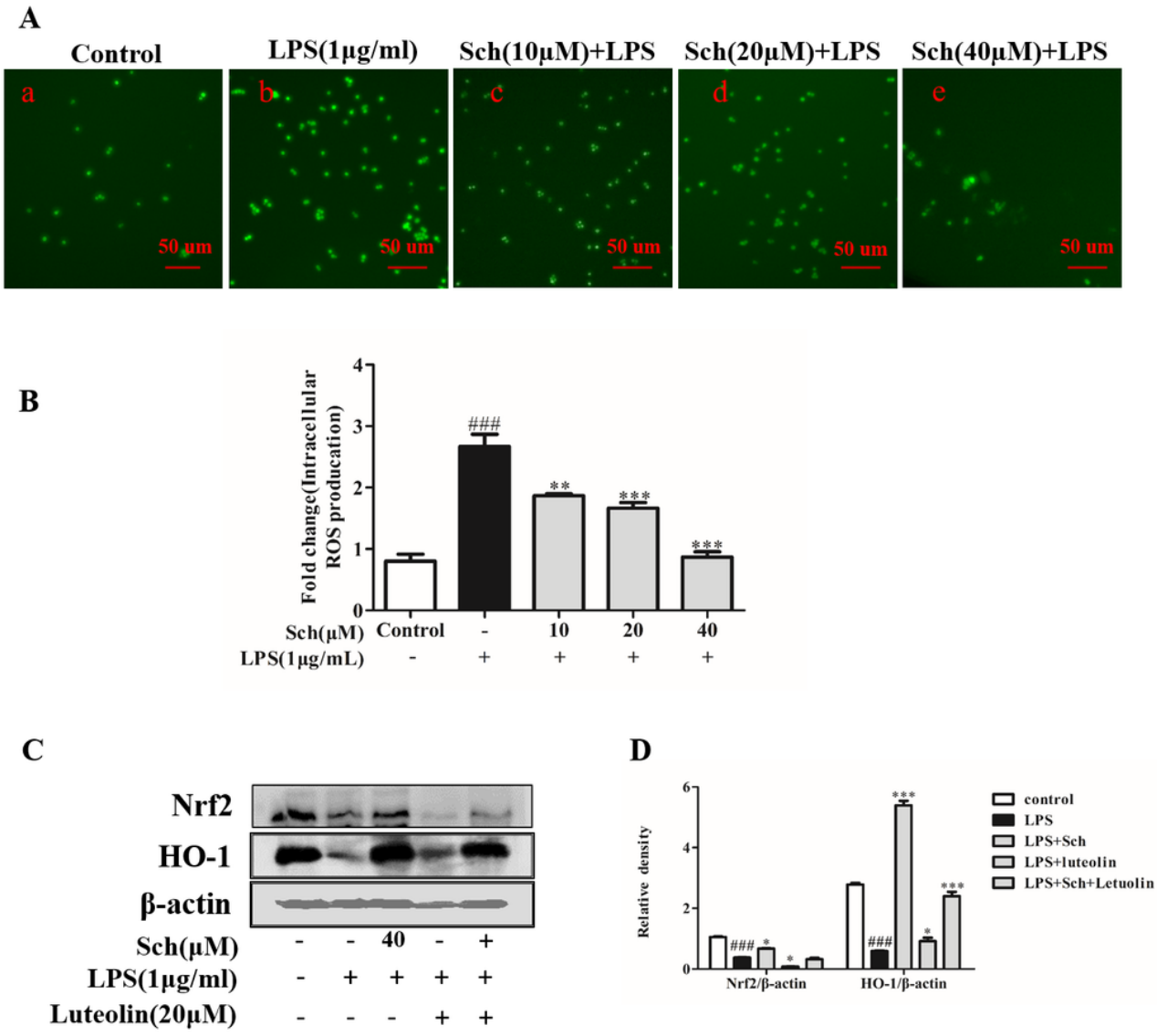

Figure 2

Effect of Sch on RAW264.7 cells viability. (A) RAW264.7 cells were pretreated with different Sch concentrations for 24 h. Using MTT assay to detect the cell viability. (B) and (C) RAW264.7 cells was pretreated with Sch (10, 20 or 40 μM) for 24 h and then LPS (1 μg/ml) was added to stimulate the cells for 24 h. ELISA was used to determine the levels of IL-6 and MCP-1 respectively. (D) RAW264.7 cells were administrated with Sch (10, 20 or 40 μM). After one day, Cells were stimulated with LPS (10 μg/ml) for 24 h. Load cells with 10 μM DCFH-DA for 1 h. Measure the production of ROS through a fluorescence microscope (magnification ×40). (E) The fold change of intracellular ROS level. Values are expressed as mean ±SEM (n=3). ###P < 0.01, ##P < 0.01 vs. the control group. **P < 0.01 and ***P < 0.001 compared with the LPS-induced group.

Fig. 3

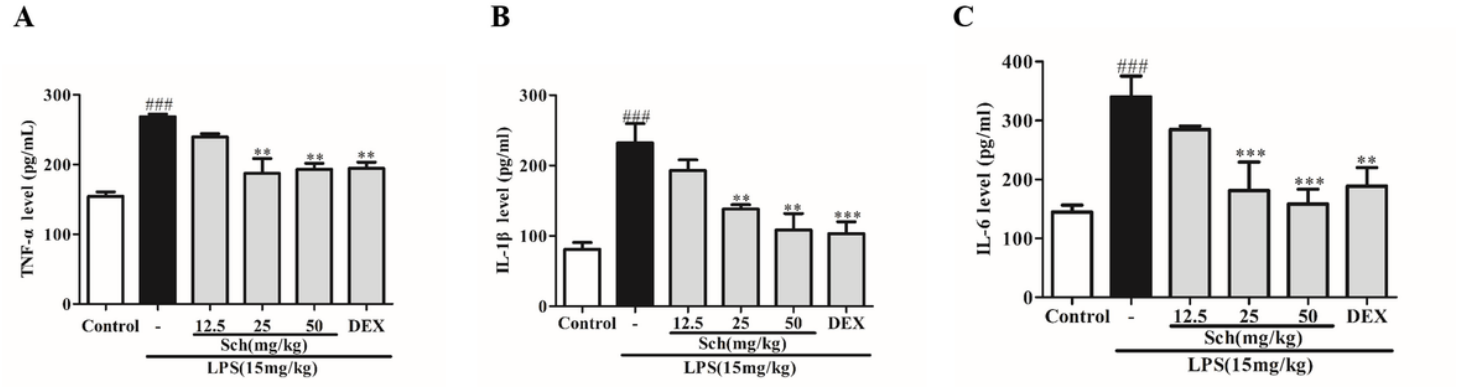

Figure 3

Effect of Sch on LPS-induced level of TNF-α, IL-1β, and IL-6 in kidney tissue. Sch (12.5, 25, or 50 mg/kg) and DEX (5 mg/kg) were administered to mice for 1 h and then stimulated with LPS (15 mg/kg) for 4 h, and serum was harvested from the mice orbit. (A) TNF-α, (B) IL-1β, (C) IL-6 were measured. Data are expressed as the mean ± SEM (n=3). ###P < 0.001 vs. the control group; **P < 0.01and***P < 0.001 vs. the LPS-induced group.

Fig. 4

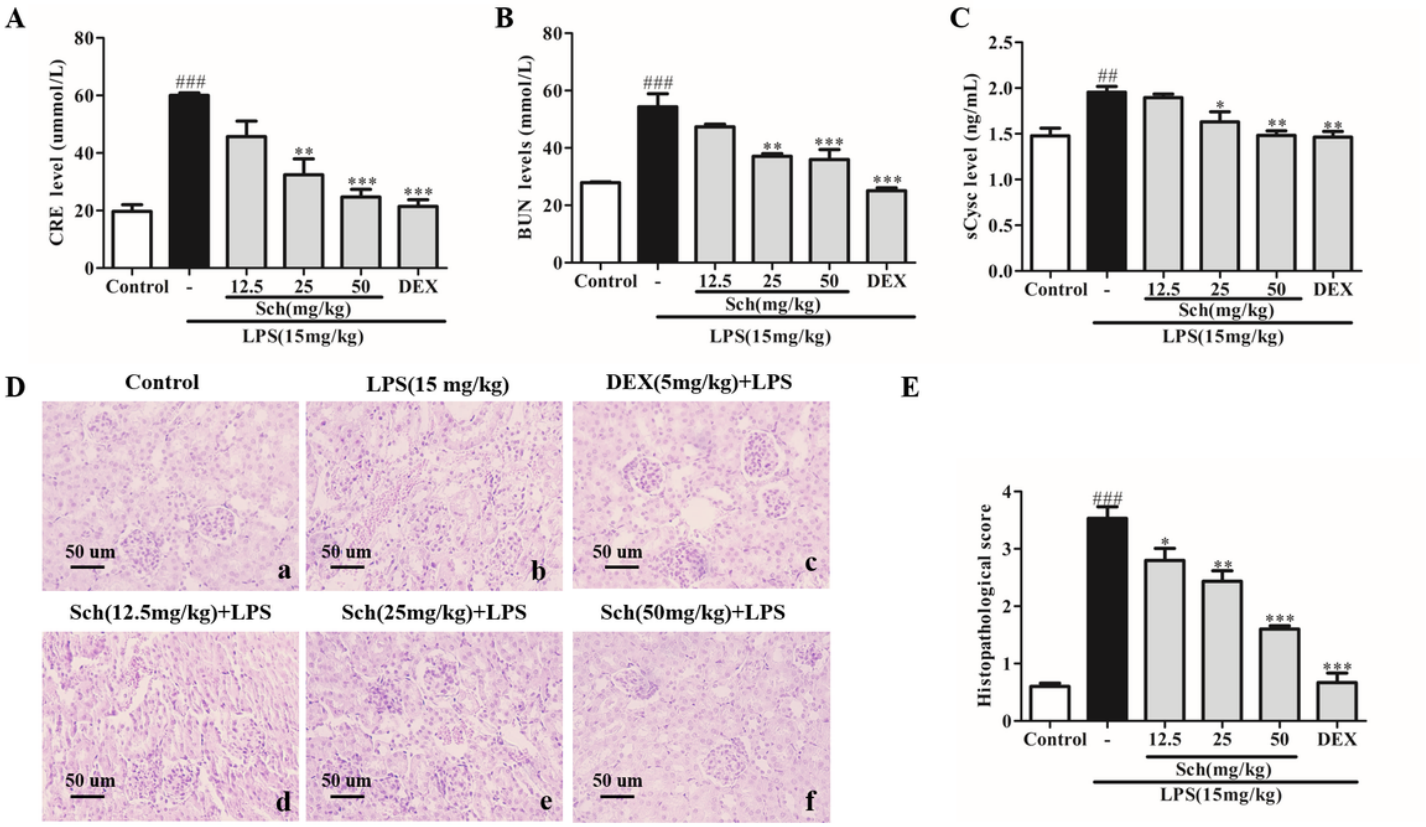

Figure 4

Effect of Sch on LPS-induced BUN, CRE and sCysC production on LPS-induced acute kidney injury in mice, as well as histopathological examination of kidney issue. One hours before the LPS administration for 4 h, Sch (12.5, 25, or 50 mg/kg) and DEX (5 mg/kg) were administered to the mice. After the LPS (15 mg/kg) challenge, blood was taken from the mice orbit and kidney tissue was obtained. (A) CRE (B) BUN and (C) sCysC in serum were tested by commercial kits, (D) and (E) Image of kidney issue. Data are expressed as the mean ± SEM (n=3). ###P < 0.001 vs. the control group; *P < 0.05, **P < 0.01 and ***P < 0.001 vs. the LPS-induced group. H&E staining of mice (magnification × 200). The criteria for evaluating kidney damage are: (0, no damage; 1, slight; 2. moderate; 3. severe; 4, very severe.

Fig. 5

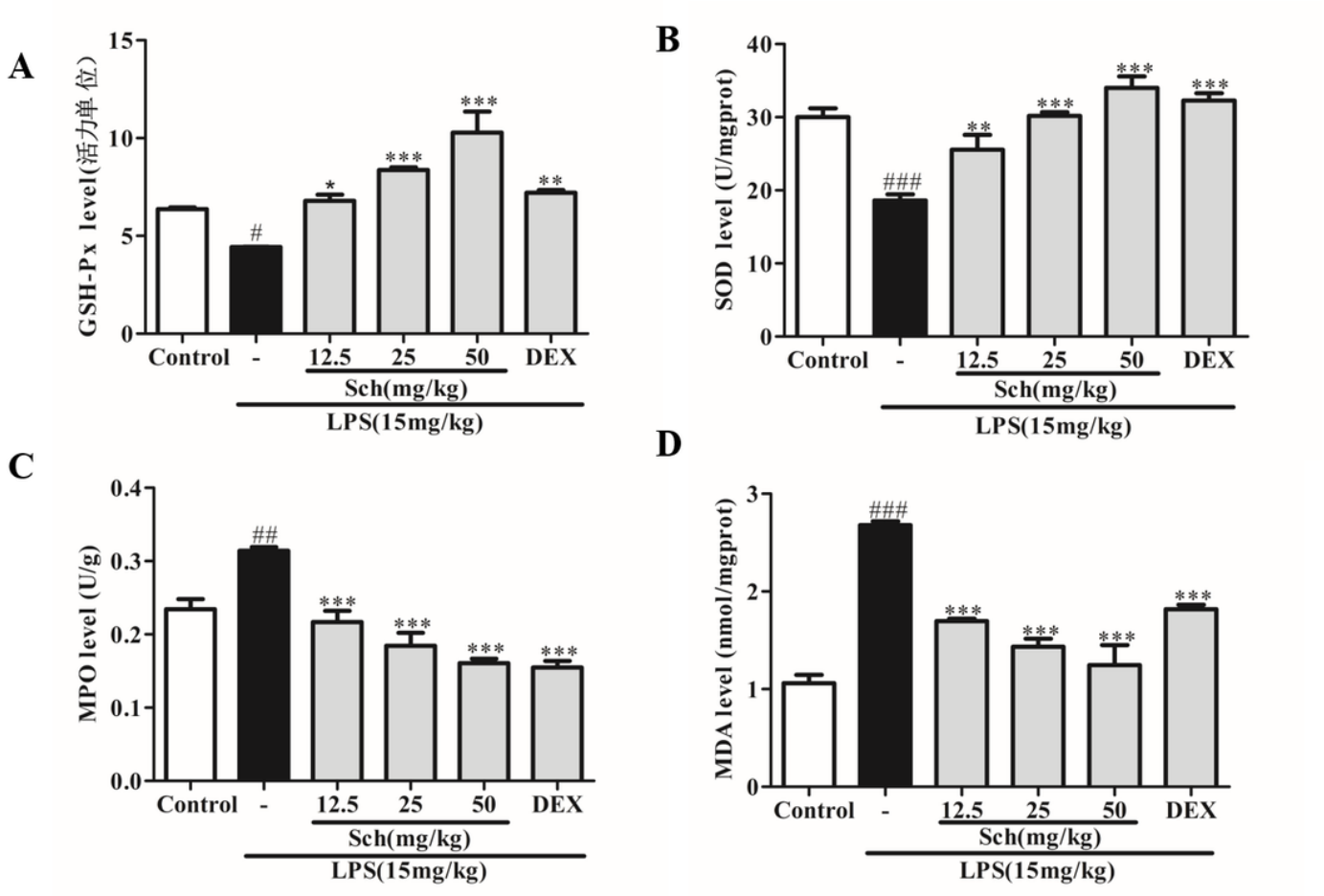

Figure 5

The effect of Sch on the levels of SOD, GSH-Px, MDA and MPO in mice with acute kidney injury induced by LPS. After administration of Sch (12.5, 25 or 50 mg/kg) and DEX (5 mg/kg), mice were intraperitoneally injected with 15 mg/kg LPS. All six groups of mice were sacrificed, and kidney tissue was obtained for tissue homogenization for measuring the levels of SOD, GSH-Px, MDA and MPO. (A) GSH-Px (B) SOD (C) MPO (D) MDA Data are expressed as the mean ± SEM (n=3). ###P < 0.001 vs. the control group; *P < 0.05, **P < 0.01 and ***P < 0.001 vs. the LPS-induced group.

Fig. 6

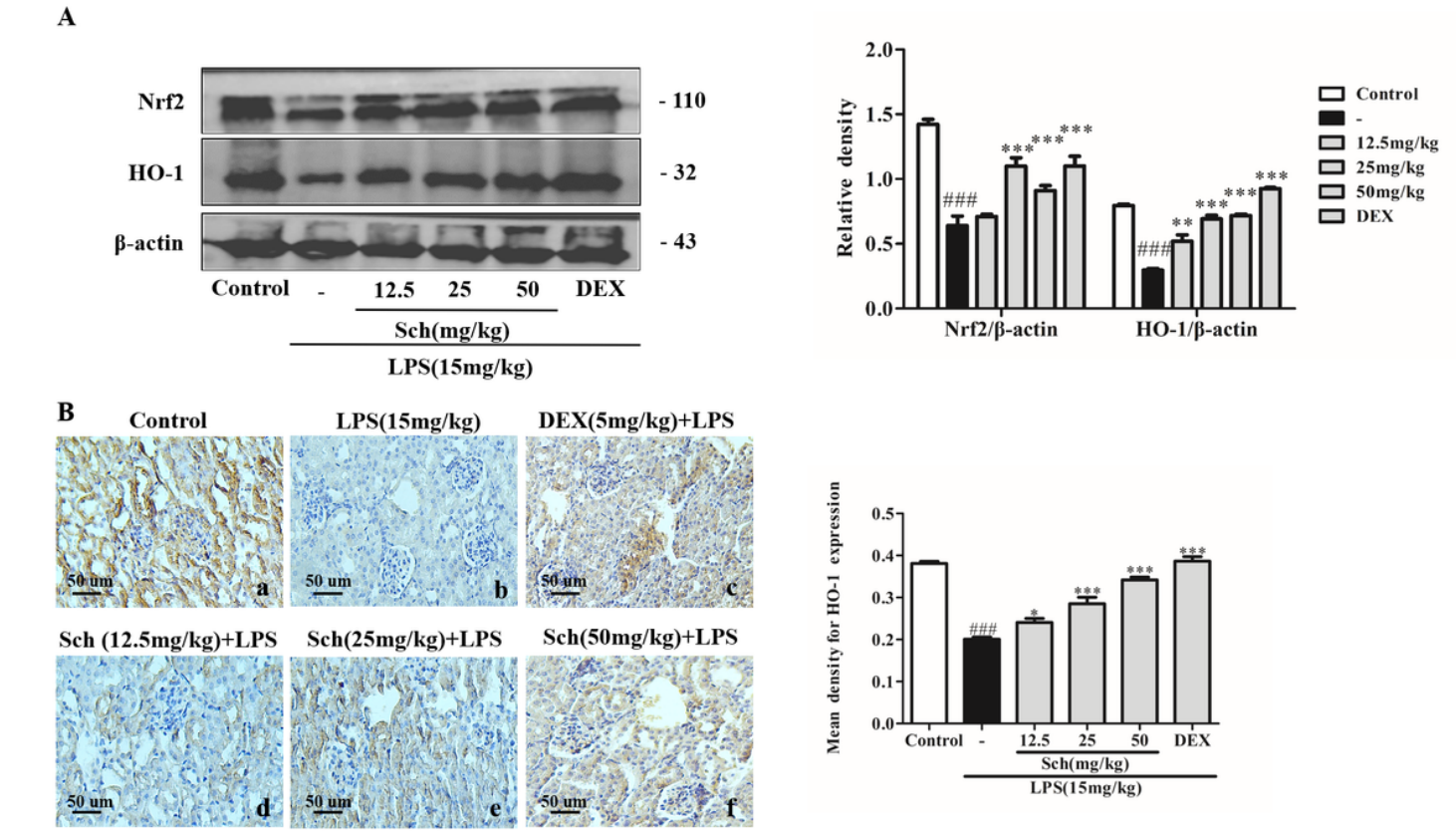

Figure 6

The expression of oxidative stress pathway related proteins in LPS-induced acute kidney injury mice. (A) Western blotting showed the expression levels of Nrf2, HO-1 and β-actin in the kidneys of mice. The treatment of Sch (12.5, 25, 50 mg/kg) and DEX (5 mg/kg) was continued for 7 consecutive days, and LPS was administered 1 h after the administration on the last day. All mice were treated 4 h later to receive tissues. The kidney was prepared as a tissue homogenate for Western blot analysis. Among them, β-actin was used as internal reference proteins. (B) Sch alleviated LPS-induced oxidative stress by immunohistochemical analysis. Magnification ×200. The data is expressed as the relative ratio of the specified protein to the internal reference protein. This part of the experiment was repeated three times. Significant difference on statistics are *P < 0.05; ***P < 0.001 vs. the control mice; ###P < 0.001 vs. the LPS-induced mice.

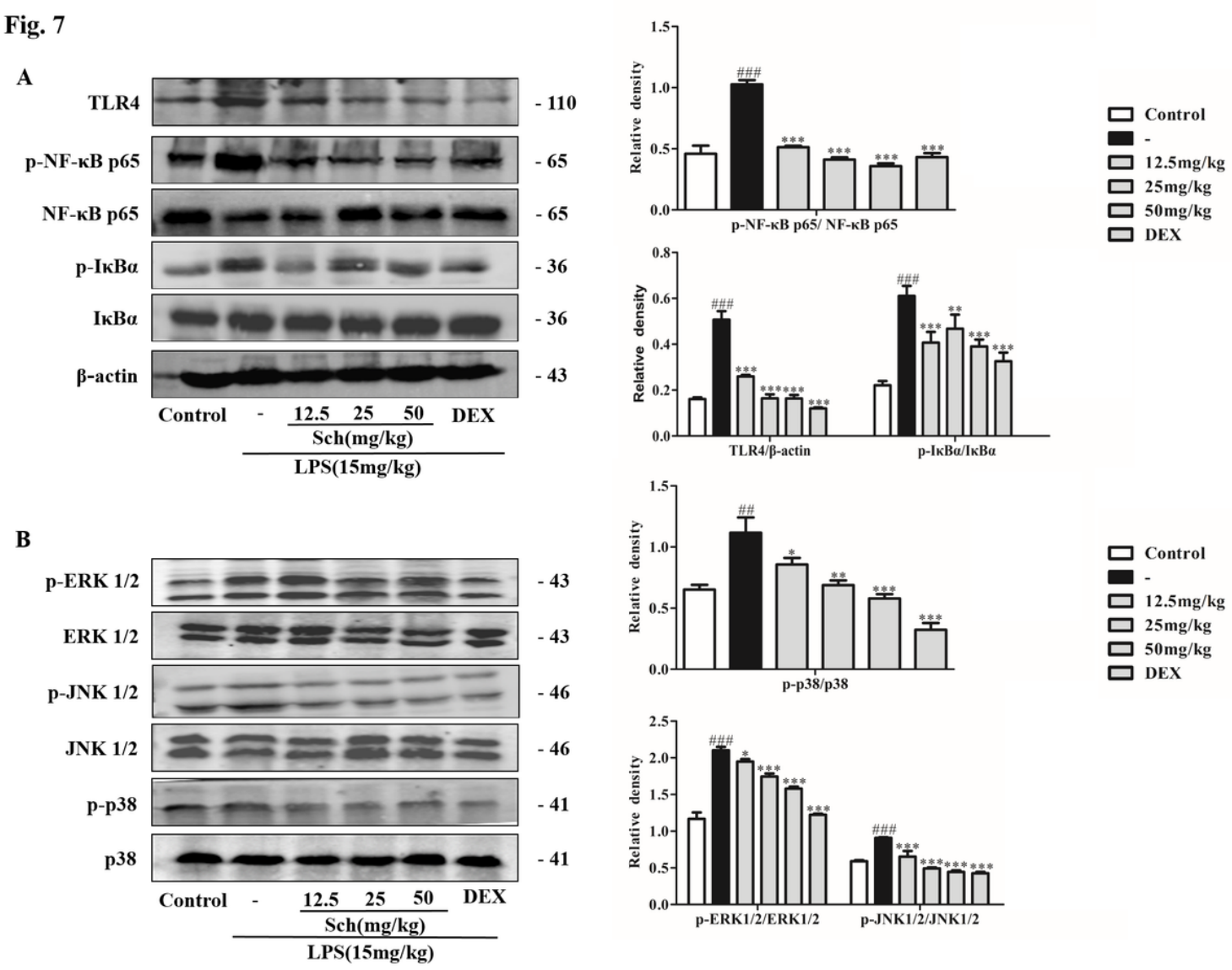

Figure 7

Sch inhibited the expression of NF-κB and MAPK inflammatory pathway proteins in kidney tissue. One hour before LPS treatment, Sch (12.5, 25, or 50 mg/kg) and DEX (5 mg/kg) were administered to the mice. After 4 h of LPS (15 mg/kg) challenge, the kidney tissue of mice was collected, and the protein was extracted for Western blot analysis. The proteins of p38, JNK1/2 and ERK1/2 are used as internal reference indicators for their corresponding phosphorylated proteins, respectively. All data are conveyed by mean±SEM (n=3). Compared with the control group, ###P < 0.001; Compared with the model group, *P < 0.05, **P < 0.01 and ***P < 0.001.

Fig. 8

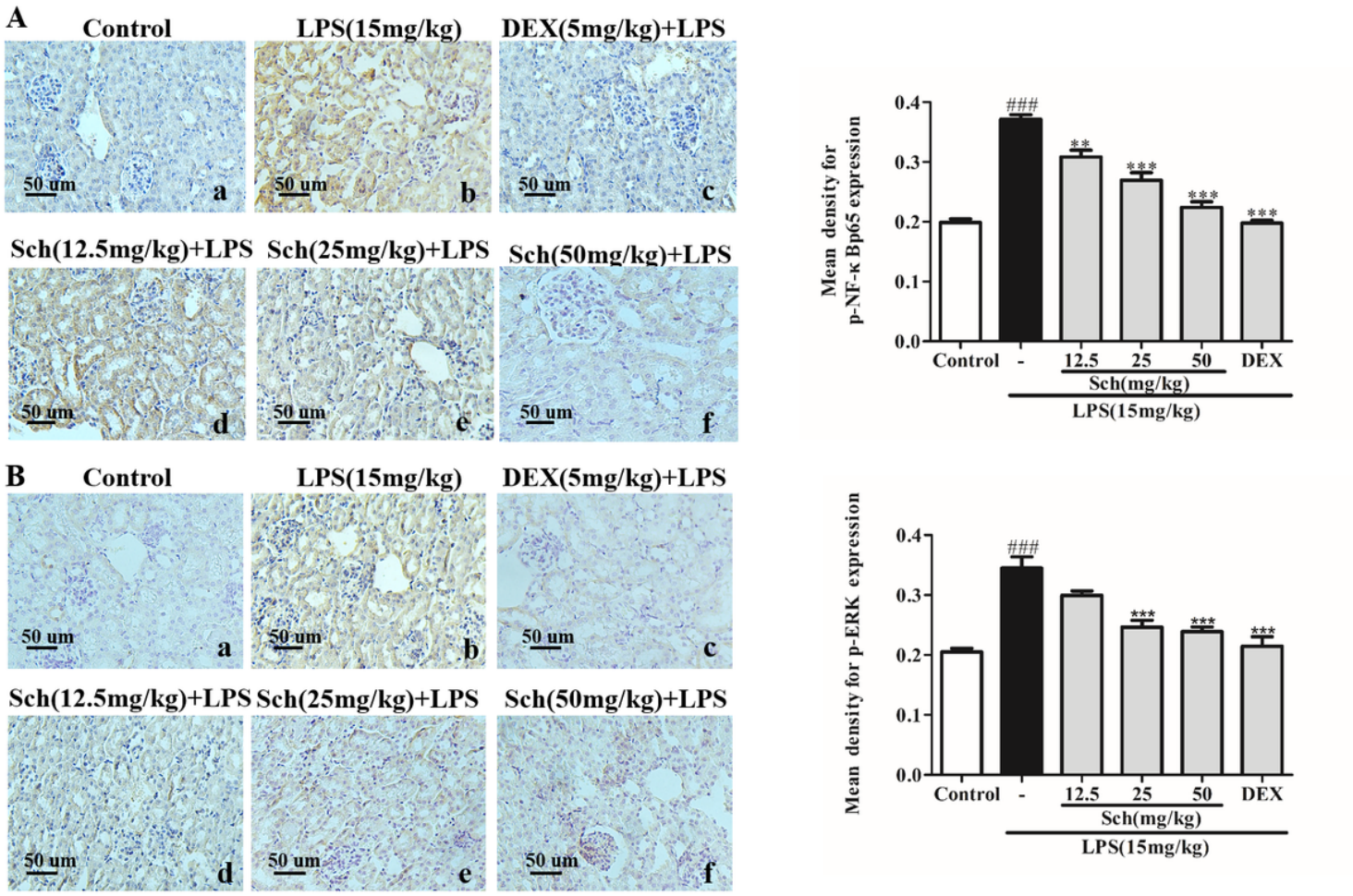

Figure 8

The effect of Sch on the expression of p-NF-κBp65 and p-ERK1/2 proteins in kidney tissue was investigated by immunohistochemistry. After 1 h of intragastric administration, LPS was stimulated for 4 h, and all mice were sacrificed to obtain kidney tissue. The concentrations of (A) p-NF-κBp65 and (B) p-ERK1/2 were collected. Magnification ×200. The brown part is a sign of a positive reaction. Data are presented as the mean ± SEM (n=3). Compared with the control group, the significant differences were ###P < 0.001, compared with the LPS-induced model group, the significant differences were *P < 0.05, **P < 0.01 and ***P < 0.001, respectively.